Pergamon

Chaos, Solitons & Fractals Vol. 10, No. 9, pp. 1491–1512, 1999

0960–0779/99/$ - see front matter

PII: S0960-0779(98)00134-9

Spatiotemporal Chaotic Dynamics of Solitons with Internal Structure in the Presence of Finite-Width Inhomogeneities

L. E. GUERRERO,[a,*] A. BELLORÍN,[b] J. R. CARBÓ[c] and J. A. GONZÁLEZ[d]

[a] Departamento de Física, Universidad Simón Bolívar, Apartado 89000, Caracas 1080-A, Venezuela
[b] Departamento de Física, Facultad de Ciencias, Universidad Central de Venezuela, Apartado Postal 47588, Los Chaguaramos, Caracas 1041-A, Venezuela
[c] Departamento de Física, Universidad de Camagüey, Circunvalación Norte, Camagüey 74650, Cuba
[d] Centro de Física, Instituto Venezolano de Investigaciones Científicas, Apartado Postal 21827, Caracas 1020-A, Venezuela

(Accepted 5 May 1998)

Abstract—We present an analytical and numerical study of the Klein–Gordon kink-soliton dynamics in inhomogeneous media. In particular, we study an external field that is almost constant for the whole system but that changes its sign at the center of coordinates and a localized impurity with finite-width. The soliton solution of the Klein–Gordon-like equations is usually treated as a structureless point-like particle. A richer dynamics is unveiled when the extended character of the soliton is taken into account. We show that interesting spatiotemporal phenomena appear when the structure of the soliton interacts with finite-width inhomogeneities. We solve an inverse problem in order to have external perturbations which are generic and topologically equivalent to well-known bifurcation models and such that the stability problem can be solved exactly. We also show the different quasiperiodic and chaotic motions the soliton undergoes as a time-dependent force pumps energy into the traslational mode of the kink and relate these dynamics with the excitation of the shape modes of the soliton.

1. INTRODUCTION

For a variety of systems the interplay between nonlinearity and disorder results in novel and fascinating phenomena [1, 2]. Particularly, the study of soliton dynamics in inhomogeneous and disordered media has received a great deal of attention in recent years [3–14] since it concerns real condensed matter systems and phenomena.

It is well known that transport properties in inhomogeneous and disordered media can change dramatically when the nonlinearity allows the creation of solitons. As a first step in the study of soliton dynamics in disordered media many authors explored the interaction between a soliton and an isolated impurity. This soliton-impurity interaction has been modeled by a point-like impurity and a structureless soliton. In real situations we can have several inhomogeneities of different kinds. When the distance between impurities is considerable higher than the width of solitons and impurities the traditional approach gives a correct result. When this is not so, we witness a series of surprising phenomena.

The dimensionless Klein–Gordon-like equations model a wide variety of soliton bearing systems [1, 2, 11, 15–31], including charge density waves, Josephson junctions, structural phase

* Corresponding author. BAMCO CCS-144-00, P.O. Box 025322, Miami, Florida, U.S.A.

transitions, crystal growth, polymers, proton conductivity, macromolecules and hydrogen-bond chains:

$$\phi_{xx} - \phi_{tt} - \frac{dU}{d\phi} = \mathscr{F}(\phi, \phi_t, x, t); \tag{1}$$

here $U = U(\phi)$ is a potential that possesses at least two minima [32], meanwhile $\mathscr{F}(\phi, \phi_t, x, t)$ represent additional forces (external forcing, dissipation, presence of impurities, inhomogeneous external fields, coupling to other degrees of freedom).

The soliton solution of eq. (1) is usually treated as a structureless point-like particle. A richer dynamics is unveiled when the extended character of the soliton is taken into account. For instance, in a previous work [6], González and Hoyst studied the ϕ^4 equation ($U = \frac{1}{8}(\phi^2 - 1)^2$:

$$\phi_{xx} - \phi_{tt} - \gamma\phi_t + \frac{1}{2}(\phi - \phi^3) = -F(x) - G(x,t). \tag{2}$$

Particularly, they showed that the zeroes of $F(x)$ (for $G \equiv 0$) play the roll of equilibrium positions for the soliton. In the case that only one zero, x_0 exists, the condition for stability for the kink/antikink is:

$$\left[\frac{\mathrm{d}F}{\mathrm{d}x}\right]_{x=x_0} \begin{cases} > 0 & \text{for the kink} \\ < 0 & \text{for the antikink.} \end{cases} \tag{3}$$

For the stable case, the inhomogeneity can trap the soliton, but in the case that $F(x)$ possesses more than one zero, the stability condition may become too complex. Here the extended character of the soliton arises, and interesting phenomena appear such as the interaction between the structure of the soliton (which is not a point-like particle) and the inhomogeneities, and between the shape modes of the soliton themselves. The external force $F(x)$ can change the spectrum of small oscillations about the soliton and additional bounded states can exist.

For the soliton of the ϕ^4 equation without perturbation, there are only two bounded states (besides the continuous spectrum): the translational mode and the shape mode. For specific values of the parameters that define the force $F(x)$ used in Ref. [6], not only an increase of the number of shape modes can exist, but in certain cases these can be unstable. Moreover the continuous spectrum can lose stability and the soliton becomes unstable against interaction with phonons.

The above mentioned authors also considered the problem with the time dependent force $G(x,t)$ and found that if $G(x,t)$ has a spatial shape such that it coincides with one of the eigenfunctions of the stability operator of the soliton, then it is possible to get resonance if the frequency of the force also coincides with the resonant frequency of the considered mode. This means, for example, that energy can be given to the translational mode (or any of the shape modes) using a $G(x,t)$ coupled to the translational mode (or any of the shape modes).

When $F(x)$ has three zeroes, this is equivalent to a double well potential (like the one found in the Duffing equation [6, 33]) chaotic motion of the soliton is possible applying an additional periodic force $G(x,t)$ for a determined set of values of the parameters.

In this paper we take into account the extended character of both the soliton and the impurity. We show that these considerations lead to the existence of a finite number of soliton internal modes that underlies a rich spatiotemporal dynamics.

We introduce impurities of the $N(x)\phi$ type, where $N(x)$ is a function with a bell shape. An impurity of this kind but using delta functions has been presented in Ref. [14]. In our paper we consider a finite width impurity and a finite width kink and show the striking differences between this approach and the traditional one (structureless solitons and delta-function-like impurities).

We present a model for which the exact stationary soliton solution in the presence of inhomogeneities can be obtained and the stability problem can be solved exactly. To achieve this purpose we solve an inverse problem in order to have external perturbations which are generic and topologically equivalent to well-known bifurcation model systems [34].

We choose the 'exact' solution such that the differential operator that appears in the stability problem is a Posch–Teller potential that can be solved exactly. Besides, the 'generated' external force and the impurities have important physical properties. In particular, the inhomogeneous force $F(x)$ is equivalent to the pitchfork bifurcation canonical form [33] and the $N(x)\phi$ impurity is topologically equivalent to the $\delta(x)\phi$ type impurity that is very frequently used.

Furthermore, we demonstrate the sensibility of the soliton internal dynamics to the inhomogeneity width even for the isolated impurity case.

Our paper is organized as follows. In Section 2 we present a description of our model and we give specific physical interpretations of the equations under consideration. In Section 3 we study the equilibrium positions of the soliton and its stability. We analyze the interaction of the soliton with the inhomogeneity created by the interplay between a finite-width and ϕ-dependent impurity and the already studied inhomogeneities independent of ϕ [6]. We also consider the action of time dependent forces fitted to the shape of the translational mode of the soliton. In Section 4 we describe the numerical simulations that confirm the theoretical results. We use the Karhunen–Loève decomposition to relate the excitation of the shape modes spectrum of the soliton with the bifurcations. In Section 5 we present the interaction of the soliton with radiation modes. Finally, in Section 6 we summarize and discuss our results and also present some concluding remarks. In the Appendices we outline the numerical method and present the Karhunen–Loève decomposition.

2. THE MODEL

The topological solitons studied in the present paper possess important applications in condensed matter physics. For instance, in solid state physics, they describe domain walls in ferromagnets or ferroelectric materials, dislocations in crystals, charge-density waves, interphase boundaries in metal alloys, fluxons in long Josephson junctions and Josephson transmission lines, etc. [11, 22].

Although some of the above mentioned systems are described by the ϕ^4-model and others by the sine-Gordon equation (and these equations, in their unperturbed versions, present differences like the fact that the sine-Gordon equation is completely integrable whereas the ϕ^4-model is not) the properties of the solitons supported by sine-Gordon and ϕ^4 equations are very similar. In fact, these equations are *topologically equivalent* and very often the result obtained for one of them can be applied to the other [22].

Here we consider the ϕ^4 equation in the presence of inhomogeneities and damping:

$$\phi_{xx} - \phi_{tt} - \gamma\phi_t + \frac{1}{2}(\phi - \phi^3) = -N(x)\phi - F(x), \tag{4}$$

where $F(x)$ is a function with (at least) one zero and $N(x)$ is a bell-shaped function that rapidly decays to zero for $x \to \pm\infty$.

In ferroelectric materials ϕ is the displacement of the ions from their equilibrium position in the lattice, $1/2(\phi - \phi^3)$ is the force due to the anharmonic crystalline potential, $F(x)$ is an applied electric field, and $N(x)$ describes an impurity in one of the anharmonic oscillators of the lattice [35]. In Josephson junctions, ϕ is the phase difference of the superconducting electrons across the junction, $F(x)$ is the external current, and $N(x)$ can describe a microshort or a microresistor [5]. In a Josephson transmission line it is possible to apply nonuniformly distributed current

sources ($F(x)$) and to create inhomogeneities of type $N(x)$ using different electronic circuits in some specific elements of the chain [11, 36].

In the present paper the functions $F(x)$ and $N(x)$ will be defined as,

$$F(x)=\frac{1}{2}A(A^2-1)\tanh(Bx), \tag{5}$$

$$N(x)=\frac{1}{2}\frac{(4B^2-A^2)}{2\cosh^2(Bx)}. \tag{6}$$

The case $F=$ *const*. has been studied in many papers (see e.g. [22]). Here eq. (5) represents an external field (or a source current in a Josephson junction) that is almost constant in most part of the chain but changes its sign in $x=0$ (this is very important in order to have soliton pinning [6]). Microshorts, microresistors and/or impurities in atomic chains [5] are usually described by Dirac's delta functions ($\delta(x)$) where the width of the impurity is neglected. The function $N(x)$ is topologically equivalent to a $\delta(x)$ but it allows us to consider the influence of the width of the impurity.

3. STABILITY ANALYSIS

Let us consider the eq. (4) and assume the existence of a static kink solution $\phi_k(x)$ that corresponds to a soliton placed in a stable equilibrium state created by the inhomogeneities $F(x)$ and $N(x)$.

Analyzing the small amplitude oscillations around the kink solution $\phi_k(x)$,

$$\phi(x,t)=\phi_k(x)+\psi(x,t), \tag{7}$$

we get, for the function $\psi(x,t)$, the following equation:

$$\psi_{xx}-\psi_{tt}-\gamma\psi_t+\frac{1}{2}(1-3\phi_k^2+2N(x))\psi=0. \tag{8}$$

Studying of the stability of the equilibrium solution $\phi_k(x)$ leads to the following eigenvalue problem (we have introduced $\psi(x,t)=f(x)\exp(\lambda t)$ into eq. (8)):

$$-f_{xx}+\frac{1}{2}(3\phi_k^2-1-2N(x))f=\Gamma f, \tag{9}$$

where $\Gamma\equiv\lambda^2-\gamma\lambda$.

Let us now study some particular cases: If $F(x)\equiv 0$, and the function $N(x)$ is described by the expression (6), then it can be shown that the exact solution for the kink in equilibrium at the position $x=0$ is,

$$\phi_k(x)=\tanh(Bx), \tag{10}$$

and that the discrete eigenvalue spectrum is described by the following formula,

$$\Gamma_n=B^2(\Lambda+2\Lambda n-n^2-2); \tag{11}$$

where the parameter Λ is defined as,

$$\Lambda(\Lambda+1)=\frac{1}{B^2}+2 \tag{12}$$

The integer part of Λ ($[\Lambda]$) defines the number of modes of the discrete spectrum.

From eq. (11) the stability condition for the translational mode ($n=0$) can be obtained:

$$4B^2<1. \tag{13}$$

It is worth noticing that if the coefficient of $N(x)$ is negative, the equilibrium position created by the impurity of the $N(x)\phi$ type is stable for the soliton, and that the stability condition is independent of the polarity of the soliton. The opposite occurs when a inhomogeneity like $F(x)$ is considered.

Furthermore, it is necessary to point out the differences between the case in which the soliton equilibrium position is due to a zero of $F(x)$, and the case in which the kink is trapped in the effective well created by the impurity $N(x)\phi$. In the former the characteristic width and the number of internal modes that can be excited are smaller than those for the free kink, and even smaller than those for the kink in equilibrium in an unstable position. While, in the latter the characteristic width and the number of internal modes that can be excited are greater than those for the free kink and for the kink in unstable equilibrium in a repulsive impurity. This is due to the inverse proportionality between the width of the impurity and B (just like the width of the kink). The impurity is more stable as B diminishes.

Finally, let us consider the case in which both types of inhomogeneities ($F(x)$ and $N(x)\phi$) are present in eq. (4). These functions are defined as in eqs. (5) and (6).

For these functions the exact solution describing the static soliton can be written:

$$\phi_k(x)=A\tanh(Bx). \tag{14}$$

The spectral problem eq. (9) brings the following eigenvalues for the discrete spectrum:

$$\Gamma_n=\frac{1}{2}A^2-\frac{1}{2}+B^2(\Lambda+2\Lambda n-n^2-2); \tag{15}$$

here Λ is defined as,

$$\Lambda(\Lambda+1)=\frac{A^2}{B^2}+2. \tag{16}$$

The stability condition for the translational mode is,

$$16B^4+2B^2(5-7A^2)+(1-A^2)^2<0. \tag{17}$$

When this condition is not fulfilled (the equilibrium position $x=0$ is unstable) and $A^2>1$, then there will exist three equilibrium points for the soliton: two stable (at points $x=x_1>0$ and $x=x_2<0$) and one unstable at point $x=0$. This happens because for large values of $|x|$ the leading inhomogeneity is $F(x)$, which is non-local and not zero at infinity. This inhomogeneity acts as a restoring force that pushes the soliton towards the point $x=0$. As a result of the competition between the local instability induced by $N(x)\phi$ at $x=0$ and the non-local inhomogeneity $F(x)$, an effective double-well potential is created. This is equivalent to a pitchfork bifurcation.

Also note that when $A=0$ then $\Lambda=1$, i.e., there is an unstable mode created by the impurity $N(x)\phi$ even for a flat initial condition. This contrasts with the $\Lambda=0$ result expected for a delta-like impurity and with the result of González and Hoyst [6] for the other kind of inhomogeneity ($F(x)$).

4. QUASIPERIODIC AND CHAOTIC SOLITONS

In this section we present numerical results for eq. (1) perturbed with inhomogeneous external forces, impurities and time-periodic forces. First, we show, for inhomogeneities of the $F(x)$ type,

the bifurcations leading to the chaotic regime. Later, we study quasiperiodic regimes as the soliton internal modes are excited by an impurity of the type $N(x)\phi$. Finally, we present bifurcations as the internal modes are excited for the case in which the two types of inhomogeneities ($F(x)$ and $N(x)\phi$) are present.

4.1. Scenario of inhomogeneous external forces

We simulate the following equation,

$$\phi_{xx}-\phi_{tt}-\gamma\phi_t+\frac{1}{2}(\phi-\phi^3)=-F(x)-G(x,t), \tag{18}$$

where static and time-dependent forces are inhomogeneous and given by the following expressions:

$$F(x)=\frac{1}{2}A(A^2-1)\tanh(Bx)+\frac{1}{2}A(4B^2-A^2)\sinh(Bx)\cosh^{-3}(Bx) \tag{19}$$

and

$$G(x,t)=v\cos(\omega t)\left(\frac{1}{\cosh^2(E(x-x_1))}+\frac{1}{\cosh^2(E(x+x_1))}\right). \tag{20}$$

The force $F(x)$, firstly introduced in Ref. [6], can be obtained as a result of an inverse problem for which an effective potential equivalent to the canonical form of the pitchfork bifurcation is desired. For $A^2>1$ and $B^2(\sqrt{1+(6A^2/B^2)}-1)<1$, we are in presence of a double-well potential *for the soliton*, (i.e., the model is a Duffing-like [33] soliton oscillator). Note that a force with three zeroes does not imply necessarily the existence of a double-well potential for the soliton.

We will attend to the dynamics of the center of mass as defined by eq. (A3). Figure 1 presents the bifurcation diagram ($A=\sqrt{\frac{3}{2}}$, $B=\sqrt{\frac{1}{10}}$, $\Lambda=2$, $\omega=1.22$, $E=0.1$, $x_1=2.5$ and $\gamma=0.450$) as the

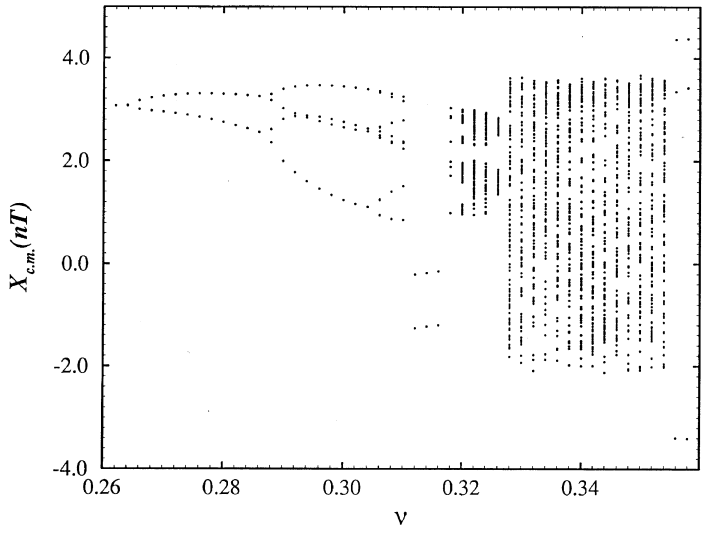

Fig. 1. Scenario of inhomogeneous external forces. Bifurcation diagram for the position of the center of mass of the kink soliton ($v=0.26...0.36$, $\gamma=0.450$).

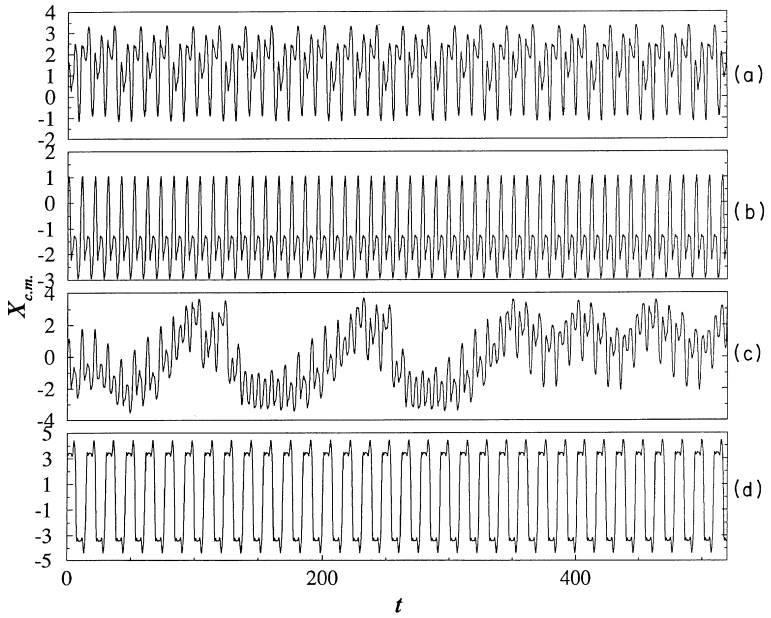

Fig. 2. Time series $x_{c.m.}$ vs t for the position of the center of mass of the kink soliton, $\gamma = 0.450$. (a) Period eight, $v = 0.310$. (b) Period four, $v = 0.312$. (c) Chaos, $v = 0.328$. (d) Period three, $v = 0.360$.

amplitude v of the time-dependent driving force is increased. The period doubling cascade for low values of the control parameter corresponds to oscillations of the soliton in one well. At $v = 0.312$ an unusual discontinuous transition interrupts the cascade: the system switches from a period-eight solution to a period-two solution but in the other well as can be appreciated in the time series presented in Fig. 2(a,b). At $v = 0.318$ the period-eight solution is recovered and a two-band regime with n-periodic (Fig. 3(a)), quasiperiodic (as the two-torus attractor presented in Fig. 3(b)) and chaotic attractors. The quasiperiodic attractor is a spatiotemporal effect: it is generated by the activation of a shape mode of the soliton which provides a frequency that is incommensurate to the driving frequency. Figures 1–2(c) reveals for $v = 0.332$ the onset of jumps of the soliton between the two wells. The regime corresponds to Duffing-like chaos for the soliton. Figure 3(b) also presents the Poincaré map which reveals the high-dimensional chaotic motion of the soliton which can be ascribed to an increased activation of shape modes (which is not possible for a Duffing-like chaotic particle). The intense activity around $x_{c.m.} = 0$ (Fig. 1) is also due to the extended character of the soliton. We have verified that at $v = 0.356$ the soliton prefers its deformation instead of its destruction and its dynamics returns to a periodic solution (Figures 1–2(d)).

Figure 4(a,b) present time series for the center of mass of chaotic solitons. In the first case ($v = 0.3$ and $\gamma = 0.505$, the rest parameters are preserved) the soliton jumps between two wells. When the damping is increased (Fig. 4(b), $\gamma = 0.550$), the soliton is constrained to move mainly in one well. Corresponding Poincaré maps (Fig. 5(a,b)) show the contrast of dimensionality (and consequently, of the number of modes and/or of the effective number of degrees of freedom) of these chaotic motions. Figure 5(c,d) present the spatiotemporal evolution for these chaotic solitons. Figure 5(c) evidences the jumps of the domain wall between the two wells, whereas Fig. 5(d) shows such a domain wall oscillating in one of the wells. Notwithstanding, note also in Fig.

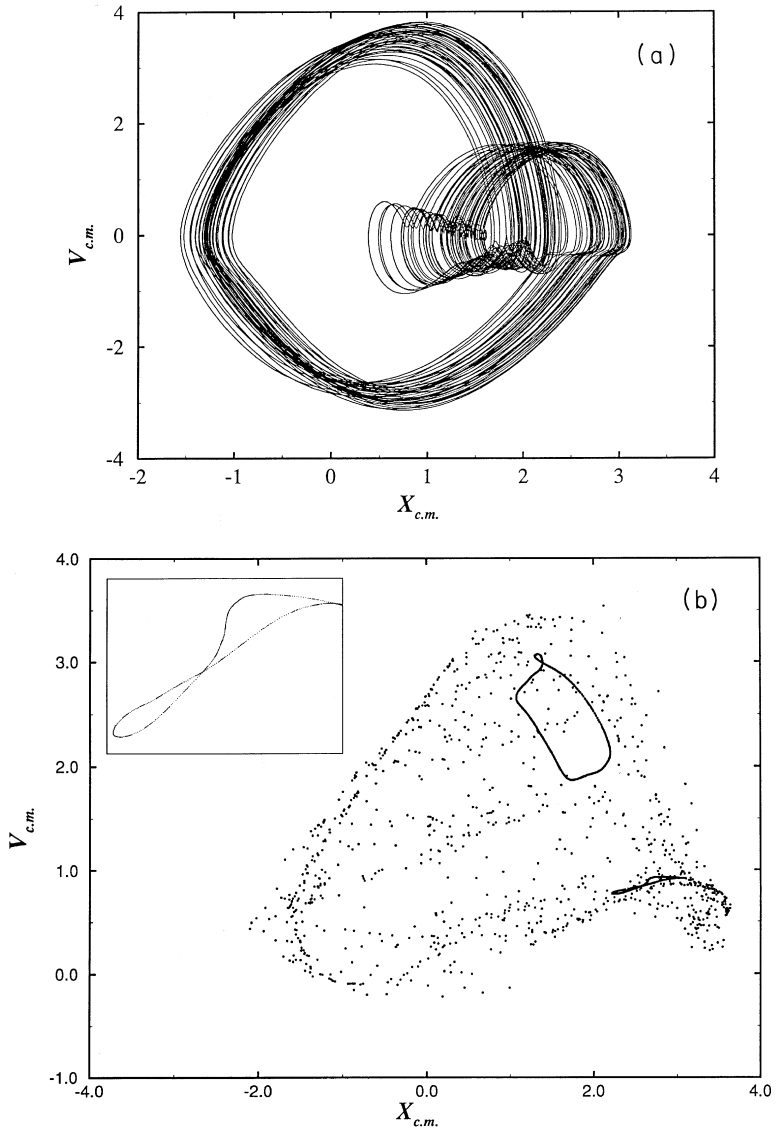

Fig. 3. Periodic, quasiperiodic and chaotic attractors, $\gamma = 0.450$. (a) Phase space $v_{c.m.}$ vs $x_{c.m.}$, $v = 0.322$. (b) Poincaré map revealing a two-torus ($v = 0.327$) and a strange attractor ($v = 0.332$). The inset presents the detail of one of the toruses.

5(d) the appearance and disappearance of deformations (depicted by yellow zones) in the other well due to tunnelling of mass/energy.

4.2. Scenario of finite-width impurity

We simulate the following model,

$$\phi_{xx} - \phi_{tt} - \gamma\phi_t + \frac{1}{2}(\phi - \phi^3) = -N(x)\phi - G(x,t), \tag{21}$$

where external forces are time-dependent and inhomogeneous. Right-hand functions are given by,

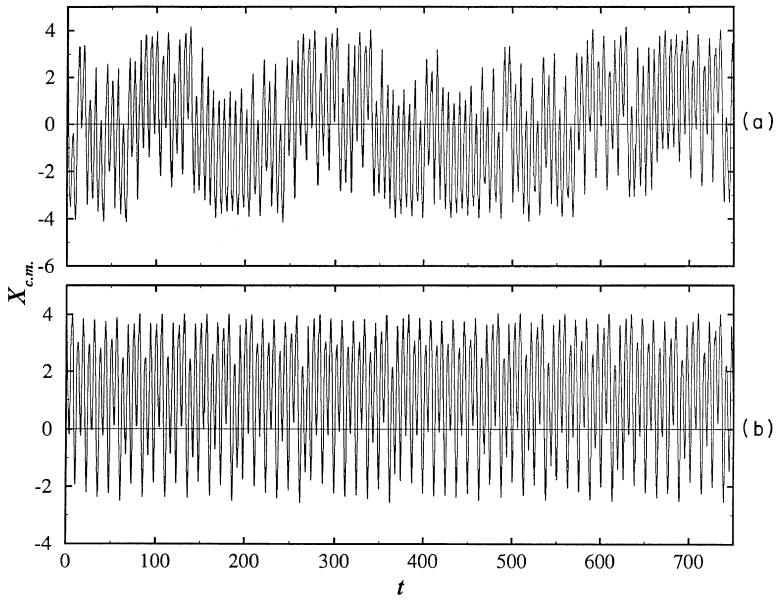

Fig. 4. Time series $x_{c.m.}$ vs t for the position of the center of mass of the kink soliton, $v=0.300$. (a) Chaotic jumps of the soliton between the two wells, $\gamma=0.505$. (b) Chaotic soliton motion mainly in one well, $\gamma=0.550$.

$$N(x)=\frac{\frac{1}{2}(4B^2-1)}{\cosh^2(Bx)} \tag{22}$$

and

$$G(x,t)=\frac{v\cos(\omega t)}{\cosh^{\Lambda}(Bx)}. \tag{23}$$

One may think that soliton dynamics in presence of an attractive impurity must be simple. Notwithstanding, that is not the case: as has been discussed in Section 3 when the width of the impurity is finite, a large number of internal modes can be excited. It can exist energy exchange between these modes and the translational mode bringing a complex dynamics.

Figure 6(a) shows the phase space for a period-three solution ($A=1.0$, $B=0.25$, $\Lambda=3.772$, $\omega=1.0$, $v=0.16$ and $\gamma=0.1$). As the amplitude v of the time-dependent driving force is increased, the excitation of an internal mode can provide a frequency incommensurate to the driving frequency, generating a two-torus quasiperiodic attractor (Fig. 6(b) for $v=0.195$, the rest parameters are the same as the previous case). On the other hand, decreasing of the damping parameter γ can provide even more incommensurate frequencies to the driving frequency as reveals the three-torus quasiperiodic motion presented in Fig. 6(c,d) for $\gamma=0.01$ and $v=0.12$.

4.3. Scenario of finite-width impurity and inhomogeneous forces

We will consider the following model:

$$\phi_{xx}-\phi_{tt}-\gamma\phi_t+\frac{1}{2}(\phi-\phi^3)=-N(x)\phi-F(x)-G(x,t), \tag{24}$$

where $N(x)$ and $F(x)$ are given by eqs. (5) and (6), and $G(x,t)$ is given by the following expressions,

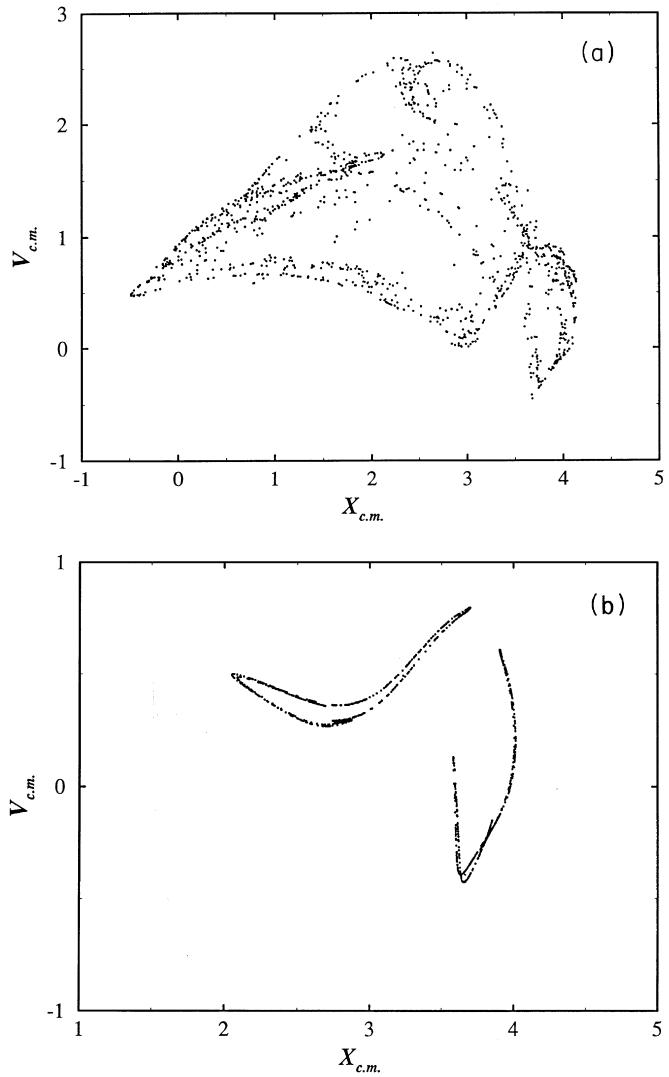

Fig. 5. Chaotic solitons, $v=0.300$. (a) Poincaré map revealing a high dimensional attractor as the soliton jumps between the two wells, $\gamma=0.505$. (b) Low dimensional attractor for kink motion mainly in one well, $\gamma=0.550$. (c,d) (continued on next page) Spatiotemporal evolution for previous attractors.

$$G(x,t)=v\cos(\omega t)\left(\frac{1}{\cosh^{\Lambda}(B(x-x_1))}+\frac{1}{\cosh^{\Lambda}(B(x+x_1))}\right). \tag{25}$$

We will study the sequence of bifurcations as the driving amplitude v is increased and other parameters remain fixed ($A=1.22$, $B=0.32$, $\Lambda=2$, $\omega=1.22$, $x_1=2.5$ and $\gamma=0.3$). Figure 7 presents the time-averaged spatial profile for different values of the amplitude v of the time-dependent driving force: $v=0.20$ (period one), $v=0.28...\ 0.45$ (quasiperiodicity), $v=0.55$ (chaos) and $v=0.60$ (period one).

Figure 8(a)–(d) present a sequence of 'quasiperiodic bifurcations': torus entangles as the amplitude of the time-dependent driving force increases and shape modes are activated.

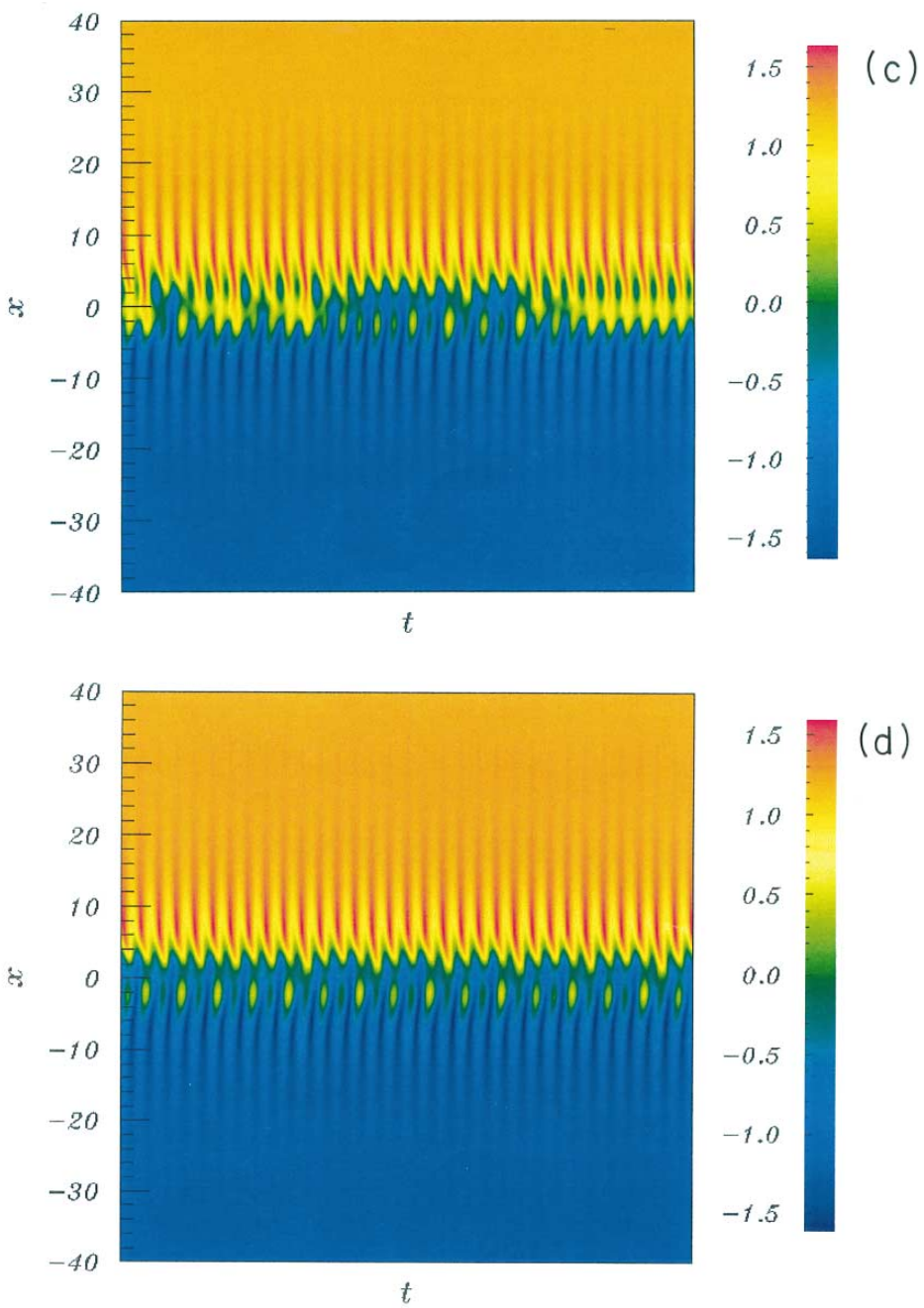

Fig. 5.—*Continued.*

Figure 9(a,b) present an chaotic soliton for $v = 0.55$. The Poincaré map (Fig. 9(a)) reveals the high-dimensional chaotic motion due to the activation of many internal modes whereas Fig. 9(a) presents the temporal evolution of the soliton and shows that the kink profile is still sustained. For these parameters the soliton is at the edge of its destruction due to the activation of the shape modes. We can consider this regime as fully developed shape chaos for the soliton.

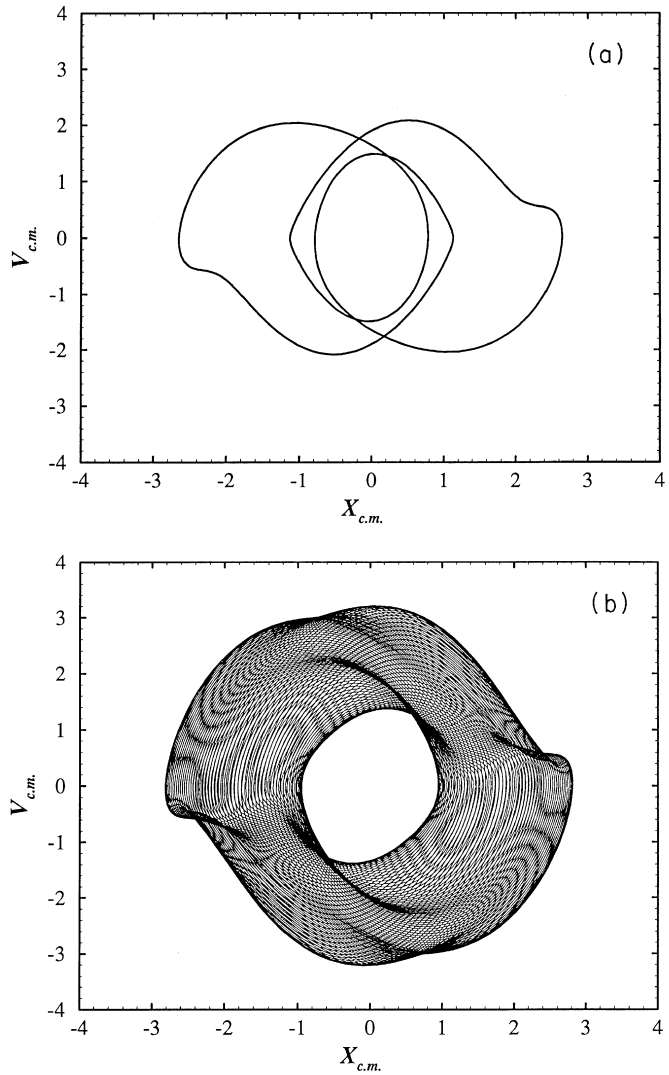

Fig. 6. Scenario of finite-width impurity. (a) Phase space $v_{c.m.}$ vs $x_{c.m.}$ for a period-three solution, $v=0.160$ and $\gamma=0.100$. (b) One-torus quasiperiodic solution, $v=0.195$ and $\gamma=0.100$. Continued on next page: (c) Phase space for a three-torus quasiperiodic solution, $v=0.120$ and $\gamma=0.010$. (d) Poincaré map for the three-torus attractor.

Along this paper we had emphasized the importance of the internal modes (or shape modes) of the soliton that can be excited as the soliton interacts with inhomogeneities. Therefore we perform a Karhunen–Loève decomposition for the sequence of dynamic attractors already presented for the scenario of finite impurity and homogeneous force.

Figure 10(a) reveals the increasing excitation of the discrete internal modes as the system evolves into a chaotic regime as well as the sudden change of the spectra for the final state that correspond to solution in which periodic motion is regained ($v=0.60$). The periodic solution for $v=0.60$ corresponds to the highest deformity of the kink profile (Fig. 7). This agrees with the higher contribution to the dynamics of the first two modes whereas all the rest of the modes decreased their contribution. Furthermore, the first shape mode replaces the translational mode

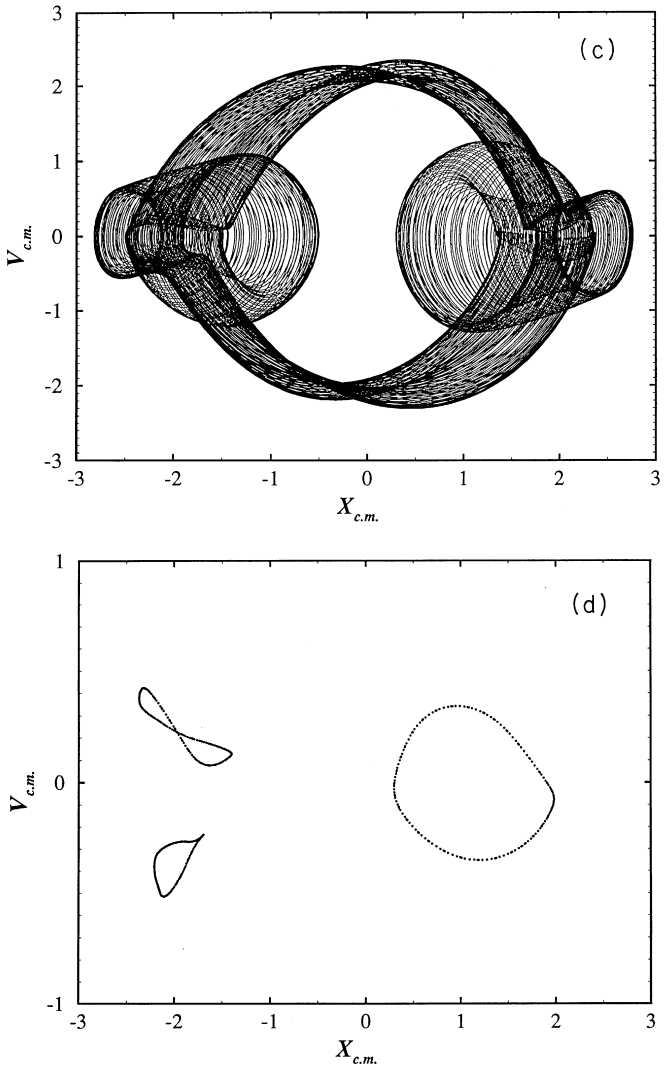

Fig. 6.—*Continued.*

as the leading mode of the dynamics. Figure 10(b) presents the leading Karhunen–Loève eigenmodes for the period-one solutions that initiates and ends the sequence of bifurcations considered in this section. The eigenmode for $v=0.20$ appears to be the superposition of a pair of translational modes centered at the equilibrium points for the soliton.

Similar situation occurs for $v=0.60$ but the eigenvalue appears to be the superposition of a pair of shape modes. Figures 11(a,b) reveal the striking difference of the temporal evolution of the period-one solitons for $v=0.20$ and $v=0.60$.

5. INTERACTION OF THE SOLITON WITH RADIATIVE MODES

Any process that involves inelastic interactions or accelerations of the soliton leads to the emission of quasi-linear waves (radiation). This phenomenon occurs by means of the modes of

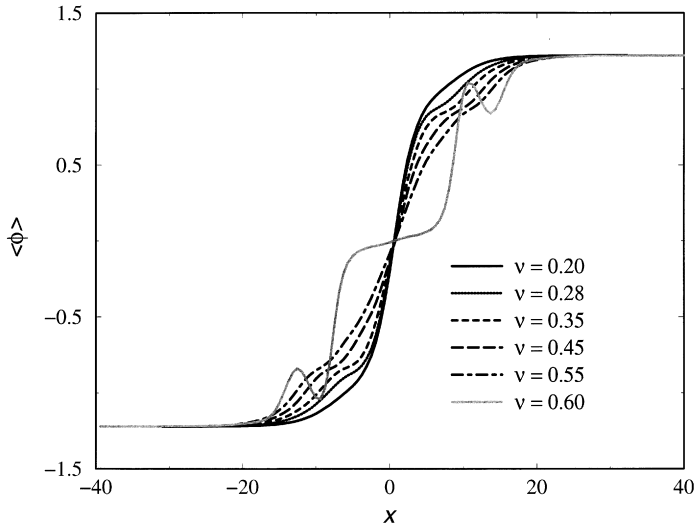

Fig. 7. Scenario of finite-width impurity and inhomogeneous forces, $\langle\phi(x)\rangle$ vs x for $v=0.20$ (period one), $v=0.28...0.45$ (quasiperiodicity), $v=0.55$ (chaos) and $v=0.60$ (period one). $\gamma=0.300$.

the continuous spectrum (radiation modes [29]) that for the case of the unperturbed ϕ^4-equation are given by

$$f_k(x)=e^{ikx}\left[3\tanh^2\left(\frac{x}{2}\right)-6ik\tanh\left(\frac{x}{2}\right)-(1+4k^2)\right]. \tag{26}$$

The interaction of a soliton with an inhomogeneity results in an emission of radiation that can be calculated using the method of McLaughlin and Scott [29] that relies on the construction of a Green's function that consists of a bilinear combination of eigenfunctions (i.e., in our case, of the eigenfunctions that we have already presented). The radiation problem also has been addressed using other perturbative methods [5].

In this paper we have focused our attention on the stability of the translational mode. Note that when the soliton is in an equilibrium position created by the impurities that is stable for the translational mode, the soliton as a whole is stable against the emission or absortion of radiation (these modes are usually called phonon modes). Moreover, in this case the kink is oscillating in an effective potential well for which radiative effects are exponentially small [5].

Notwithstanding, we remark that when the equilibrium position is unstable the shape modes can also become unstable (under certain conditions) and this can destroy the soliton. Moreover, under a certain condition the modes of the continuous spectrum can also be unstable. This is very surprising as it leads the soliton to be unstable against the emission and the absortion of radiation modes. This interesting effect is shown in Fig. 12 where we present the interaction of a radiation mode with the soliton under instability conditions for the continuous spectrum. The usual methods for calculating the radiation can not give this result. For instance, the phenomenon shown in Fig. 12 is produced by the evolution of the system

$$\phi_{xx}-\phi_{tt}-\gamma\phi_t+\frac{1}{2}(\phi-\phi^3)=-F(x), \tag{27}$$

$$F(x)=B(4B^2-1)\tanh(Bx) \tag{28}$$

under initial conditions that represent the superposition of a radiation mode and a soliton,

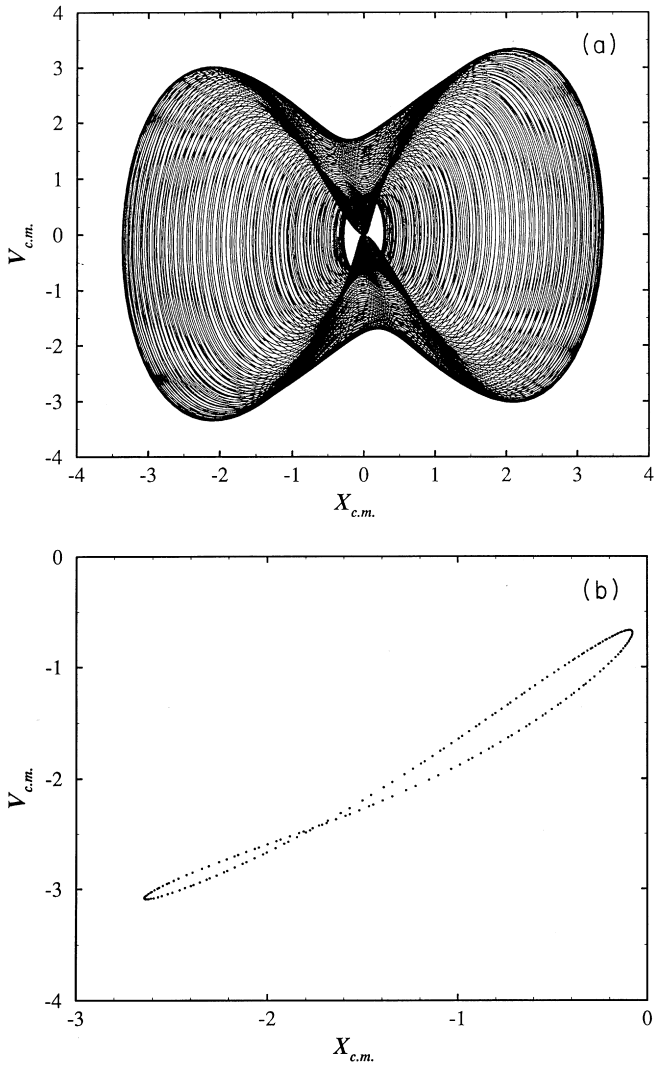

Fig. 8. Scenario of finite-width impurity and inhomogeneous forces: quasiperiodic bifurcations, $\gamma = 0.300$. (a,b) Phase space and Poincaré map for $v = 0.280$. Continued on next page: (c,d) Phase space and Poincaré map for $v = 0.350$.

$$\phi(x,0) = 2B\tanh(Bx) + C\{3\sin(Bx)\tanh(Bx) - 6\cos(Bx)\tanh(Bx) - 5\sin(Bx)\}, \tag{29}$$

$$\phi_t(x,0) = 0 \tag{30}$$

For $4B^2 - 1 < 0$ the translational mode is unstable. For $10B^2 - 1 < 0$ the first shape mode also becomes unstable. Moreover, for $12B^2 - 1 < 0$ the soliton becomes unstable against the interaction with radiation modes (Fig. 12).

In Fig. 13 we present the case $4B^2 > 1$. Here the amplitude of radiation mode is greater than the case presented in Fig. 12. Notwithstanding, the original shape of the kink is recovered.

The continuous spectrum (which concerns with radiation) was considered in our calculations and numerical experiments. In the numerical experiments there are emission of radiation that is absorbed by the resistance (dissipative terms).

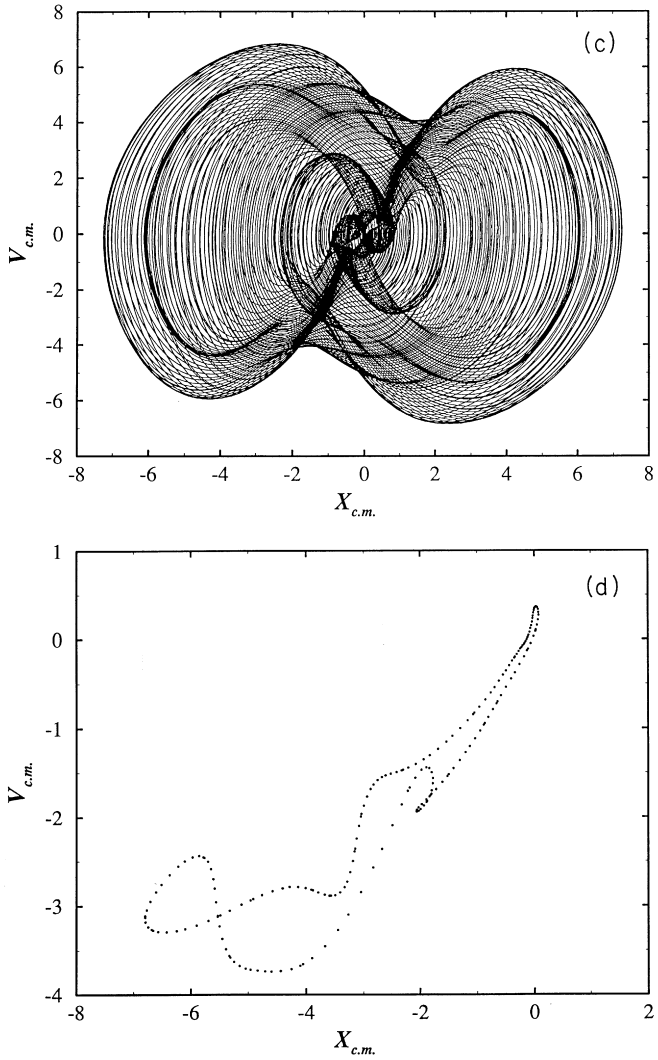

Fig. 8.—*Continued.*

When the soliton is trapped the translational mode has a relevant role in contrast with the case for which the free soliton enters in interaction with an impurity. For the last case the shape modes indeed play a determinant mode.

6. SUMMARY AND CONCLUSIONS

In this paper we have presented the importance of considering the soliton as an extended particle as it interacts with real inhomogeneous media.

We have shown that a finite-width impurity can activate a large number of soliton internal modes. In fact, for an impurity of the $N(x)\phi$ type with a stable point the number of mode increases (as the width of the impurity increases) in comparison with the free soliton case. Surprisingly, this contrasts with the inhomogeneous external force $F(x)$ with a stable point case,

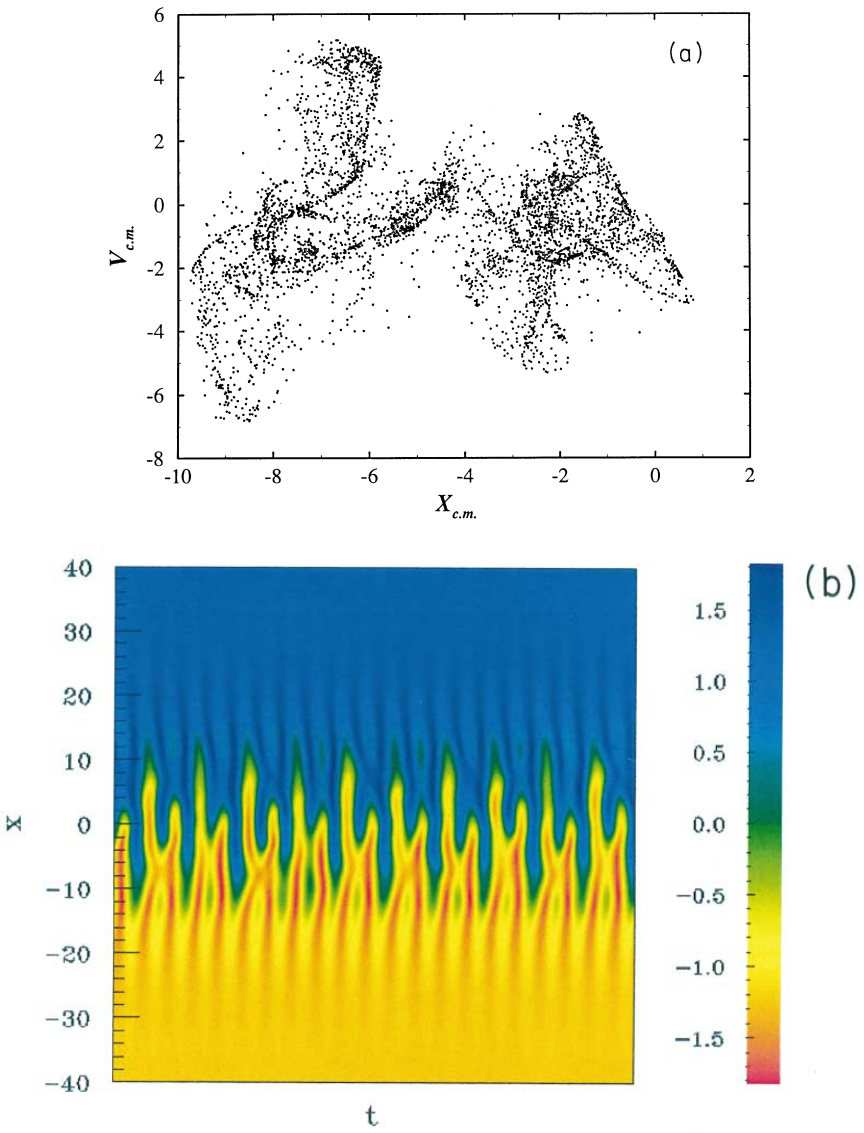

Fig. 9. Shape chaos, $\gamma = 0.300$ and $v = 0.550$. (a) High dimensional Poincaré map. (b) Spatiotemporal evolution.

where the opposite occurs. An interesting finite-size effect occurs when both inhomogeneities, $F(x)$ and $N(x)\phi$, exhibiting only one equilibrium point when considered individually, generate a double-well effective potential for the soliton as they interact between each other and with the soliton.

In addition, we have predicted surprising effects when more than one impurity is considered. For instance, the stability condition depends on a variety of parameters that we can control (i.e., the width and the height of the impurity as well as the width of the soliton) and which we present as very relevant to the whole dynamics.

We have shown the importance of the internal modes of the soliton as they can generate shape chaos for the soliton as well as cases in which the first shape mode leads the dynamics.

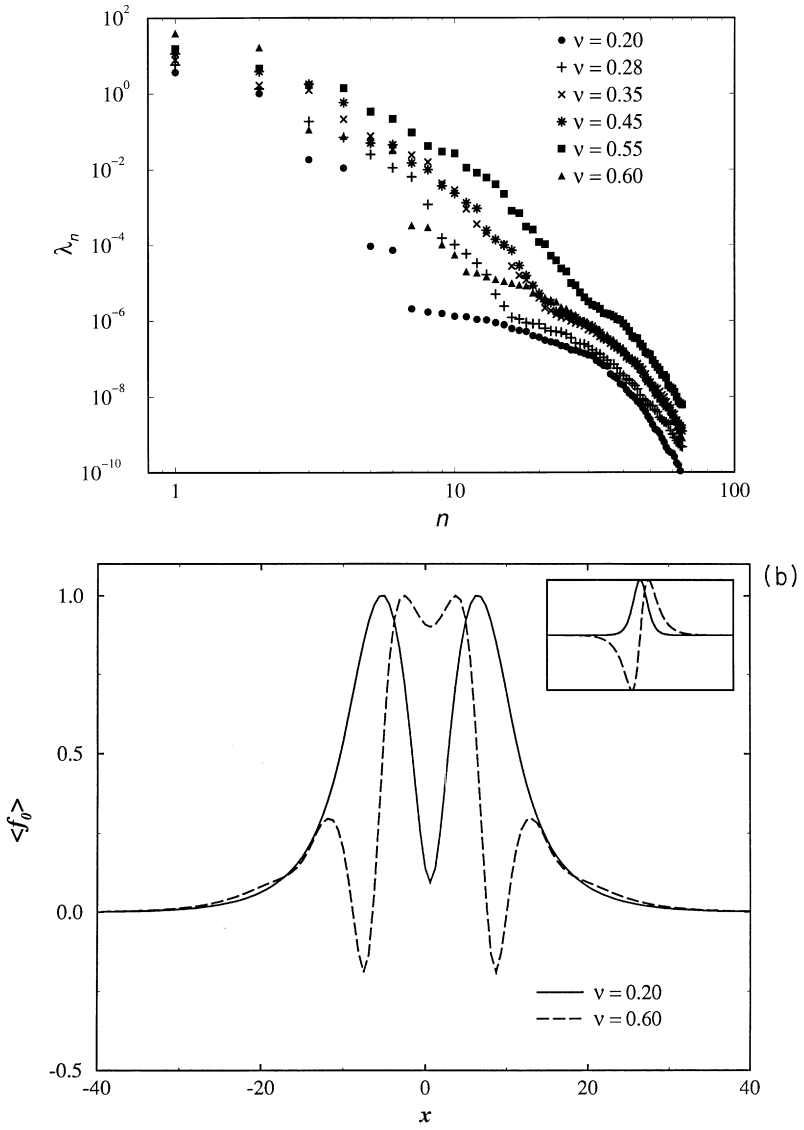

Fig. 10. (a) Karhunen–Loève spectra for the sequence of bifurcations presented in Fig. 7. (b) Plot of the first mode of the Karhunen–Loève spectrum for $v = 0.20$ and $v = 0.60$. The inset shows the translational mode and the first shape mode.

Our approach has been also applied to the stochastic resonance [37] of solitons that can oscillate in a double-well potential [38]. Our approach provides the possibility to encounter resonances linked to the different internal modes of the soliton as well as to tune the time-dependent driving force to a selected mode.

The results presented in this paper are very relevant for the concrete physical systems presented in Section 2. as they concern the pinning problem (i.e., the stability problem of the soliton in an equilibrium point created by the inhomogeneities). As we have seen, it is not trivial to determine whether the equilibrium position is stable or not for the soliton when we are in the presence of external fields and inhomogeneities having finite widths and, also the extended character of soliton is considered. Real experiments [39, 40] where this kind of phenomena has been observed

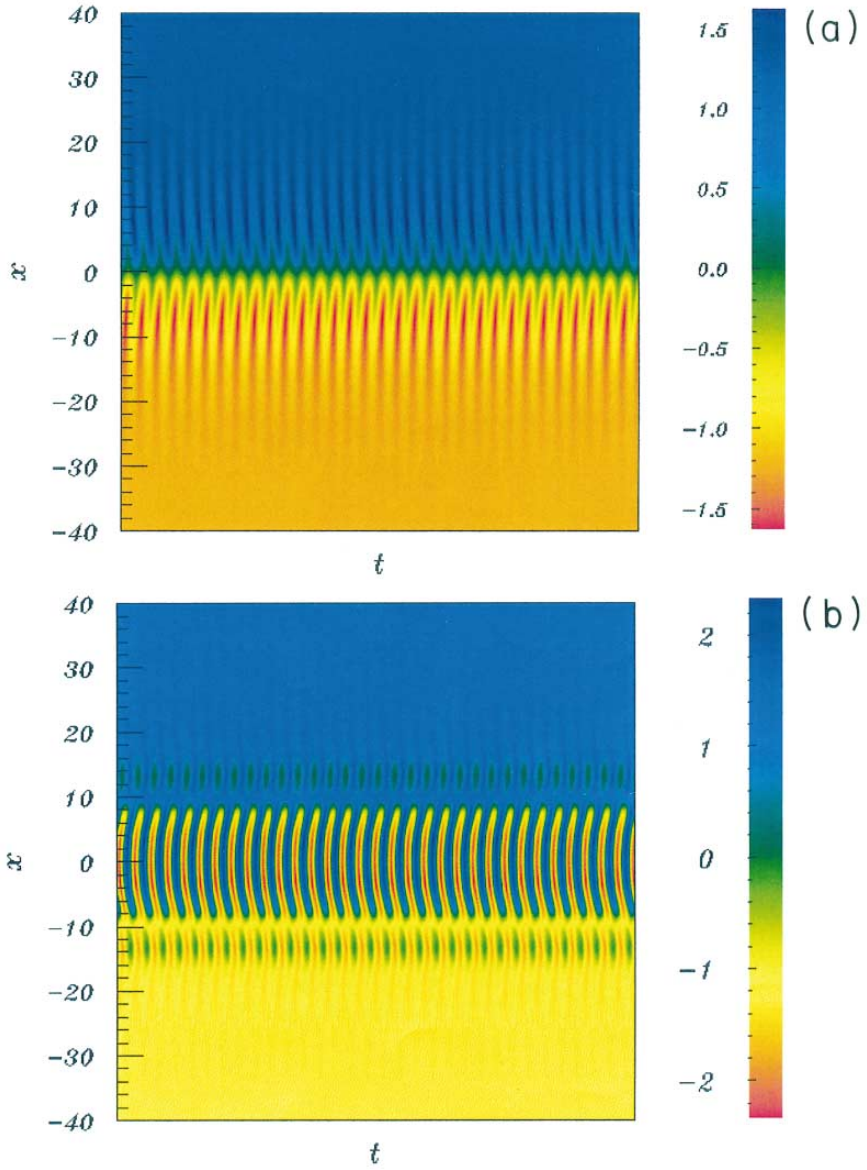

Fig. 11. (a)–(b) Spatiotemporal evolution of the period one solutions that initiates and ends the sequence of bifurcations presented in Fig. 7.

show that, in certain cases, the description of the impurities using delta functions can lead to erroneous conclusions.

Soliton oscillators in Josephson junctions have been studied intensively in the last years due to their application as sources of radiation [41]. In this context the study presented in this paper of the sustained oscillations of a soliton in an effective potential well has great importance. Grøbech-Jensen and Blackburn [42] have studied a system of coupled Josephson junctions as a super-radiant power source. Their point is that the oscillator ceases to be a point-like oscillator and exhibits a spatial degree of freedom. This leads to a radiation power greater than the expected

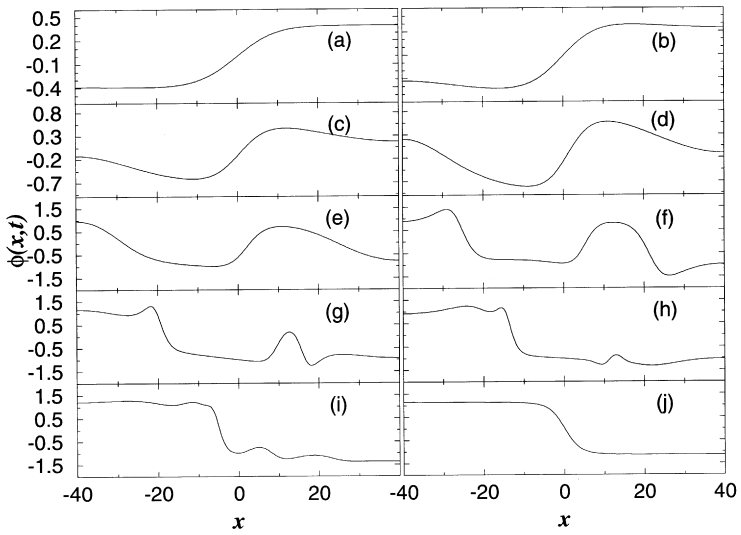

Fig. 12. (a)–(j) Interaction of the soliton with radiation modes: soliton explosion. After the explosion an anti-kink is formed. Note that the initial kink profile is stretched because the equilibrium position is unstable whereas the opposite occurs for the final stage. ($L=80$, $\gamma=0.1$, $B=0.2$ and $C=-0.001$).

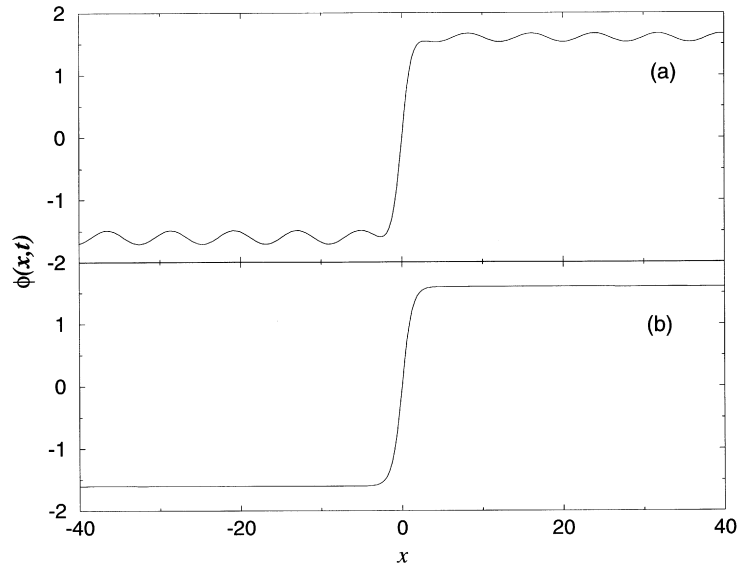

Fig. 13. (a,b) Interaction of the soliton with radiation modes under stability conditions for the continuous spectrum. The amplitude of the radiation mode is greater than the case presented in Fig. 12 as is evident in the snapshot (a) for $t=0$ ($L=80$, $\gamma=0.1$, $B=0.8$ and $C=-0.011$).

from the point-like oscillators theory. In this paper we have shown that under the effects of the inhomogeneities the soliton exhibit an internal spatial degree of freedom. Furthermore, there is an increased number of activated internal modes. Particularly, we have shown that for impurities of the type $N(x)\phi$ with a stable equilibrium position, the hyperradiant effect could be achieved varying the impurity width. In this case the width of soliton will be greater than the width of the unperturbed soliton. This is also valid for impurities of the type $N(x)\sin\phi$ which can describe a

microshort in a sine-Gordon-like systems. The chaotic oscillations and the soliton explosion phenomenon (due to soliton instability against the interaction with radiation modes) can be also important for the design of soliton based devices.

Acknowledgement—This work has been partially supported by Consejo Nacional de Investigaciones Científicas y Tecnológicas (CONICIT) under Project S1-2708.

REFERENCES

1. Bishop, A. R., Campbell, D. K. and St. Pnevmatikos (eds). *Disorder and nonlinearity*. Springer-Verlag, Berlin, 1989.
2. Abdullaev, F. Kh, Bishop, A. R. and St. Pnevmatikos (eds). *Nonlinearity with disorder*. Springer-Verlag, Berlin, 1992.
3. Abdullaev, F. Kh., *Theory of solitons in inhomogeneous media*, John Wiley and Sons, New York, 1994.
4. Konotop, V. V. and Vázquez, L. *Nonlinear random waves*. World Scientific, Singapore, 1995.
5. Kivshar, Y. S., Malomed, B. A. *Rev. Mod. Phys*., 1989, **61,** 763, and references therein.
6. González, J. A., Hoyst, J. A.. *Phys. Rev. B*., 1992, **45,** 10338.
7. Kivshar, Yu. S., Zhang, F., Vázquez, L. *Phys. Rev. Lett*., 1991, **67,** 1117.
8. Zhang F., Kivshar, Yu. S. and Vázquez, L. *Phys. Rev. A*., 1992, **45**, 6019; *Phys. Rev. A*., 1992, **46**, 5214.
9. Zhang, F., Konotop, V. V., Peyrard, M., Vázquez, L. *Phys. Rev. E*., 1993, **48,** 548.
10. Sánchez, A., Bishop, A. R. *Phys. Rev. E*., 1994, **49,** 4603.
11. González, J. A., Guerrero, L. E., Bellorin, A. *Phys. Rev. E*., 1996, **54,** 1265.
12. González, J. A., de Mello, B. *Physica Scripta*, 1996, **54,** 14.
13. Remoissene, M. and Peyrard (eds). *Nonlinear coherent structures in physics and biology*, *lecture notes in physics*, Vol. 393. Springer-Verlag, Berlin, 1991.
14. Kivshar, Yu. S., Sánchez, A. and Vázquez, L. In *Nonlinear coherent structures in physics and biology*, eds. M. Remoissenet and M. Peyrard. Springer-Verlag, Berlin, 1991.
15. Hänggi, P., Talkner, P., Borkovec, M. *Rev. Mod. Phys*., 1990, **62,** 251.
16. Aubry, S. *J. Chem. Phys*., 1975, **62,** 3217.
17. Krumhansl, J. A., Schriefer, J. R. *Phys. Rev. B*., 1975, **11,** 3535.
18. Bishop, A. R., Domany, E., Krumhansl, J. A. *Ferroelectrics*, 1977, **16,** 183.
19. Collins, M. A., Blumen, A., Currie, J. F., Ross, J. *Phys. Rev. B*, 1979, **19,** 3630.
20. Rice, M. A., *Phys. Lett. A*., 1979, **71**, 152; *Phys. Lett. A*, 1979, **73**, 153.
21. Campbell, D. K., Bishop, A. R. *Nucl. Phys. B*., 1982, **200,** 297.
22. Bishop, A. R., Krumhansl, J. A., Trullinger, S. E. *Physica D*., 1980, **1,** 1.
23. Fisher, D. S. *Phys. Rev. B*., 1985, **31,** 1396.
24. St. Pnevmatikos. *Phys. Lett. A*., 1987, **122,** 249.
25. Gordon, A. *Physica B*, 1987, **146,** 373.
26. Lu, Y., *Solitons and polarons in conducting polymers*. World Scientific, Singapore, 1988.
27. Lonngren, K. and Scott, A. (eds). *Solitons in action*. Academic, New York, 1978.
28. Coppersmith, S. N. *Phys. Rev. Lett*., 1990, **65,** 1044.
29. McLaughlin, D. W., Scott, A. C. *Phys. Rev. A*, 1978, **18,** 1652.
30. Krug, J. and Spohn, H., *Europhys. Lett*., 1989, **8**, 219; Krug, J., *Phys. Rev. Lett*., 1995, **75**, 1795.
31. Guerrero, L. E., López Atencio, E., González, J. A. *Phys. Rev. E*, 1997, **55,** 7691.
32. González, J. A., Hoyst, J. A. *Phys. Rev. B*, 1987, **35,** 3643.
33. Guckenheimer, J. and Holmes, P. J., *Nonlinear oscillations, dynamical systems and bifurcations of vector fields*. Springer-Verlag, Berlin, 1986.
34. Zeeman, E. C., *Catastrophe theory: selected papers*. Addison-Wesley, Reading, Massachusetts, 1977.
35. Collins, M. A., Blumen, A., Currie, J. F., Ross, J. *Phys. Rev. B*, 1979, **19,** 3630.
36. Landauer, R. *J. Appl. Phys*., 1980, **51,** 5594.
37. Benzi, R., Sutera, A. and Vulpiani, A., *J. Phys. A*., 1981, **14**, L453; Bulsara, A. R. and Gammaitoni, L., *Physics Today*, 1996, **49**, 39.
38. González, J. A., Mello, B. A., Reyes, L. I., Guerrero, L. E. *Phys. Rev. Lett*., 1998, **80,** 1361.
39. Itzler, M. A. and Tinkham, M., *Phys. Rev. B*, 1995, **51**, 435; *Phys. Rev. B*, 1995, **51**, 9411.
40. Itzler, M. A., private communication.
41. Costabile, G., Pagano, S., Pedersen, N. F. and Russo, M. (eds). *Nonlinear superconductive electronics and Josephson devices*. Plenum Press, New York, 1991.
42. Grønbech-Jensen, N., Blackburn, J. A. *Phys. Rev. Lett*., 1993, **70,** 1251.
43. Karhunen, K., Ann. Acad. Sci. Fennicae, Ser A1, *Math. Phys*., 1946, **37**; Loève, M. M., *Probability Theory*, Van Nostrand, Princeton, 1955.
44. Sirovich, L., *Physica D*, 1989, **37**, 126; Knight, B. and Sirovich, L., *Phys. Rev. Lett*., 1990, **65**, 1365.
45. Ciliberto, S., Nicolaenko, B. *Europhys. Lett*., 1991, **14,** 303.
46. Guerrero, L. E., Hasmy, A., Mata, G. J. *Physica B*, 1994, **194–196,** 1631.

APPENDIX A. NUMERICAL METHOD

We have integrated our ϕ^4-like equations using a standard implicit finite difference method with open boundary conditions $\phi_x(0,t)=\phi_x(l,t)=0$ and a system length $l=80$.

We use a kink-soliton as initial condition:

$$\phi(x,0)=A\tanh\left[\frac{B(x-x_0)}{\sqrt{1-v_0^2}}\right] \tag{A1}$$

and

$$\phi_t(x,0)=\frac{-ABv_0}{\sqrt{1-v_0^2}}\cosh^{-2}\left[\frac{B(x-x_0)}{\sqrt{1-v_0^2}}\right], \tag{A2}$$

here A and B are constants whereas $x_0=1.0$ and $v_0=0$ are the initial position and velocity of the center of mass of the soliton.

We define the position of the center of mass of the kink-soliton as,

$$x_{c.m.}=\frac{\int_{-l/2}^{l/2}x\phi_x^2\mathrm{d}x}{\int_{-l/1}^{l/2}\phi_x^2\mathrm{d}x}. \tag{A3}$$

APPENDIX B. THE KARHUNEN–LOÈVE DECOMPOSITION

The Karhunen–Loève decomposition [43–46] allows to describe the dynamics in terms of an adequate basis of orthonormal functions or modes. The field $\omega(x,\,t)$ to be decomposed represents the fluctuations of $\phi(x,t)$ with respect to the time-averaged spatial pattern $\phi_{ave}(x)$. We find a basis of orthonormal functions $\Psi_n(x)$ by solving an integral equation whose kernel is the two points correlation function $K(x,x')=\langle\omega(x,t)\omega(x',t)\rangle$ (here $\langle\ldots\rangle$ means time average). The functions $\Psi_n(x)$ are the eigenfunctions of the integral equation,

$$\int_0^L K(x,x')\Psi_n(x')dx'=\lambda_n\Psi_n(x). \tag{B1}$$

The eigenvalues λ_n can be regarded as the weight of the mode n.